Investigation of pilot-scale 8040 FO membrane module under different operating conditions for brackish water desalination

Jung Eun Kim, Sherub Phuntsho, Fezeh Lotfi, Ho Kyong Shon*

School of Civil and Environmental Engineering, University of Technology, Sydney (UTS), Post Box 129, Broadway, Sydney, NSW 2007, Australia, email: Hokyong.Shon-1@uts.edu.au (H.K. Shon)

ABSTRACT

Two spiral wound forward osmosis membrane modules with different spacer designs (corrugated spacer [CS] and medium spacer [MS]) were investigated for the fertilizer-drawn forward osmosis (FO) desalination of brackish groundwater (BGW) at a pilot-scale level. This study mainly focused on examining the influence of various operating conditions such as feed flow rate, total dissolved solids (TDS) concentration of the BGW feed, and draw solution (DS) concentrations using ammonium sulfate ($(NH_4)_2SO_4$, SOA) on the performance of two membrane modules. The feed flow rate played a positive role in the average water flux of the pilot-scale FO membrane module due to enhanced mass transfer coefficient across the membrane surface. Feed TDS and DS concentrations also played a significant role in both FO membrane modules because they are directly related to the osmotic driving force and membrane fouling tendency. CS module performed slightly better than MS module during all experiments due to probably enhanced mass transfer and lower fouling propensity associated with the CS. Besides, CS spacer provides larger channel space that can accommodate larger volumes of DS, and hence, could maintain higher DS concentration. However, the extent of dilution for the CS module is slightly lower.

Keywords: Forward osmosis; Brackish groundwater; Spiral-wound module; Optimization; Fertigation

1. Introduction

Forward osmosis (FO) has recently attracted widespread interest because the driving force in FO process is provided by the concentration gradient between the concentrated draw solution (DS) and the feed water. Thus, the energy consumption in FO is comparatively lower than current pressure-driven membrane processes such as reverse osmosis (RO). The potential application of FO process has been investigated for many different industries such as wastewater treatment, seawater desalination, and food industries [1]. However, FO process is largely influenced by the concentration polarization (CP) effects, reverse salt flux (RSF), and properties of both FO membrane and DS [2].

*Corresponding author.

Although a variety of FO membrane studies have been conducted at a bench-scale level using a flat sheet FO membrane [3–5], research using large-scale spiral-wound membrane module is still limited [6]. It must be acknowledged that the results from the lab-scale experimental studies are not adequate to identify some of the specific FO performances in terms of the recovery of feed and flux behaviors [7]. Recently, the performance of a spiral-wound 4040 FO membrane module (i.e. 4 inch for the diameter and 40 inch for the length) was studied for the first time and identified under different operating conditions [7]. The FO membrane module used in this previous study was a standard element, which had a medium spacer (MS) made of diamond-type polypropylene spacer. From this experimental approach for analyzing the structure features of a spiral-wound FO module, the relationships between water flux and operating conditions were initially identified and optimized.

Spiral-wound module (SWM) has been used in many areas such as desalination and waste water treatment because of its high membrane area to volume ratio and a good balance between operation, fouling control, and permeate rate [8]. The performance of a SWM is influenced by many factors such as the number of leaves, feed and permeate channel heights, mass transfer, and raw feed water conditions [8,9]. SWM contains a flow channel for the feed surrounded by membrane sheets with active membrane layers facing the flow path. It is normal for the membrane sheets to have barrier layers contacting each other and separated by a spacer as a turbulence promoter in the feed flow channel [10].

In addition, DS properties play a crucial role in the performance of FO process because the net osmotic driving force is generated by the concentration difference between the feed solution (FS) and DS. Therefore, the selection of DS will be guided by many factors such as osmotic pressure, water solubility, and molecular weight [11]. Many different DSs have been applied for the FO process depending on applications, including inorganic- and organic-based DS, magnetic nanoparticles, and concentration RO brine [11]. Among these draw solutes, inorganic-based fertilizers have been introduced and selected as a DS for the FO process in order to produce irrigation water using saline water as FS. This concept of fertilizer-drawn FO (FDFO) desalination process was introduced and examined in our previous studies [12–15]. The rationale behind this concept is that the diluted fertilizer DS after FO desalination can be directly applied to the plants as it is an essential component of the plant growth. This avoids the need for the separation of draw solutes and the desalted water after the FO

process, which is one of the challenges when FO is applied for the desalination to produce potable water [12].

In this work, we investigated the comparative performances of the two spiral wound forward osmosis (SWFO) membrane modules at a pilot-scale level for the desalination of brackish groundwater (BGW) using a fertilizer as DS. Two modules were made up of different spacers and spacer thicknesses, and their performances were comparatively investigated in terms of water flux under different operating conditions that included feed flow rate, total dissolved solids (TDS) of the BGW, and DS concentration. This work aims to establish the ability to produce water flux under different conditions, thus providing a basis for further long-term test operations of the modules.

2. Experimental methods

2.1. 8040 SWFO membrane module

A schematic diagram of SWM is shown in Fig. 1. Each FO membrane sheet is separated by the feed flow spacer and membrane sheets with the spacers in between are glued together. The permeate flux extracted from feed water dilutes the DS and is collected inside the central tube. Two different 8040 SWFO modules were employed (Hydration Technology Innovations, Albany, OR), and the number 8040 indicates the diameter of 8 inch and the length of 40 inch. Both SWFO membrane modules were made up of cellulose tri acetate (CTA) FO membranes. As shown in Table 1, 8040 FO CS module (referred to as corrugated spacer [CS] module) has a CS made up of 2.5 mm polystyrene chevron and an effective membrane area of 9 m^2 with six membrane leaves. 8040 FO MS module (referred to as MS module) has a MS made of 1.14 mm diamond-type polypropylene screen and an effective membrane area of 11.2 m^2 with seven
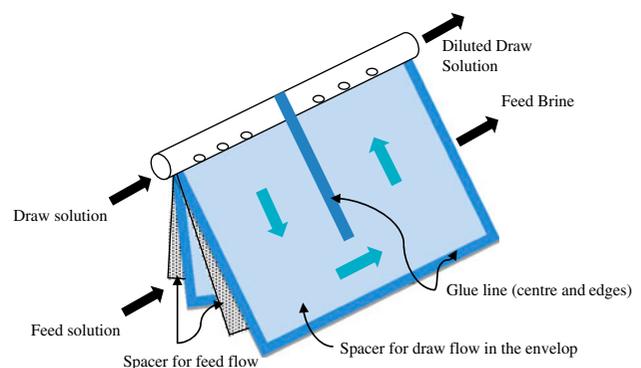
Fig. 1. An illustration of SWFO membrane module.

Table 1
Specifications of 8040 SWFO membrane module (Hydration Technology Innovations, Albany, OR)

SWFO module	Useable membrane area (m^2)	Membrane leaves	Spacer (mm)
8040 FO CS module	9.0	6	2.5—Corrugated spacer (polystyrene chevron flow path)
8040 FO MS module	11.2	7	1.14—Medium spacer (diamond type polypropylene)
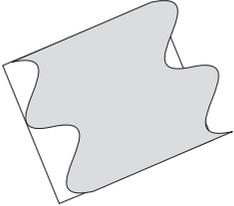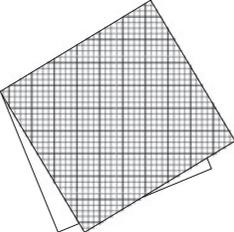
membrane leaves. For both FO membrane modules, the pressure drop correlation was provided by FO membrane module manufacturer (HTI). The active layer of the membrane is against the FS and the porous support layer of the membrane faces the DS. Each SWFO module was loaded inside a polyvinyl chloride vessel.

2.2. Feed and draw solutions

For initial baseline test of both FO modules, tap water pre-treated by microfiltration (MF) was used as feed water and 5% sodium chloride (NaCl) was used as DS to compare the water flux provided by membrane manufacturer. The pre-treated tap water was used for preparing all FD and DS. The initial volumes of feed water and DS were 200 and 100 L, respectively.

FS for all experiments were prepared by dissolving unprocessed salt produced from the evaporation of BGW in the Murray–Darling Basin (MDB) in the pre-treated tap water. Three different TDS concentrations of feed water were prepared: 5, 10, and 35 g/L (BGW5, BGW10, and BGW35, respectively). The composition of the unprocessed salt used in this study is shown in Table 2 and it was analyzed using inductively coupled plasma mass spectrometry (ICP-MS

PerkinElmer ELAN DRC-e). In addition, ammonium sulfate ((NH_4)$_2SO_4$ or SOA) of 0.6, 0.8, and 1.0 M was used as the DS for this study because of relatively higher water flux and lower RSF among all selected

Table 2
Compositions of salt produced from the evaporation pond in the MDB

Compounds	Concentration
Bicarbonate alkalinity (soluble) (mg/kg) (as HCO_3)	100
Arsenic (mg/kg)	<1
Lead (mg/kg)	<1
Manganese (mg/kg)	11
Zinc (mg/kg)	1
Iron (%)	<0.01
Aluminum (%)	<0.01
Boron (mg/kg)	<1
Calcium (mg/kg)	2,249
Magnesium (mg/kg)	789
Potassium (mg/kg)	27
Sodium (mg/kg)	352,866
Sulfur (mg/kg)	1,860
Phosphorus (mg/kg)	1
Total dissolved solids (mg/kg)	357,904
Osmotic pressure (bar, at 25℃)	281.86

Table 3
FS and DS used in the pilot-scale FDFO process operation. Osmotic pressures of both solutions were determined by OLI Stream Analyzer 3.2 (OLI Systems Inc., Morris Plains, NJ, US)

Feed solution	Concentration (g/L)	Total dissolved solids (TDS, ppm)	Osmotic pressure π (atm)
BGW BGW5	5	3,950	3.11
BGW10	10	7,290	5.74
BGW35	35	22,800	17.92
Draw solution	MW	Concentration (M)	Osmotic pressure π (atm)
NaCl	58.5	0.85	95.01
$(NH_4)_2SO_4$ or SOA	132.1	0.6	28.12
		0.8	37.11
		1.0	46.14

fertilizers in our previous studies [12,15]. The osmotic pressure of both FS and DS (in Table 3) was calculated using OLI Stream Analyzer 3.2 (OLI System Inc., Morris Plains, NJ, US).

2.3. Pilot-scale FDFO membrane module setup

A schematic diagram of the pilot-scale FDFO system for BGW desalination is illustrated in Fig. 2. Firstly, MF is used as a pre-treatment process to remove the particulate compounds in raw feed water

that could affect the FO membrane performance. For FDFO operation, the BGW feed comes in contact on one side of the membrane (active layer) and the concentrated DS on the other side of the membrane (support layer). The FDFO process was operated in the batch mode in which both the DS and FS after passing through the FO modules are recycled back to their respective tanks. Therefore, the concentration of DS decreased, while the TDS of the feed increased with time. FO membrane module has two different types of ports: two side ports and two end ports. The side ports refer to the usual high-pressure side of the elements and thus the feed water was pumped through these ports. The end ports refer to the unpressurized side of the element and the DS is fed from these ports. The feed flow rate varied from 50 to 100 LPM (litre per minute), while draw flow rate was maintained at 0.5 LPM during the whole experiment. Physical cleaning of the pilot-scale FDFO system was conducted using the pre-treated tap water for at least 3 h. After each cleaning, baseline flux was determined using pre-treated tap water as FS and 5% NaCl as DS.

According to the concept of FDFO desalination process [12], the diluted fertilizer DS is directly applied for irrigation because it contains fertilizer nutrients essential for the plants. Nevertheless, it has been observed that the nutrient concentration of the diluted DS is higher than the required concentration and this concentration depends on the feed TDS. Therefore, as mentioned earlier, this pilot-scale system is composed of NF as a post-treatment process to reduce the final fertilizer nutrient concentration for direct fertigation of crops (as shown in Fig. 2). NE 4040-90 SWM (Woongjin Chemical Co. Ltd, Korea)
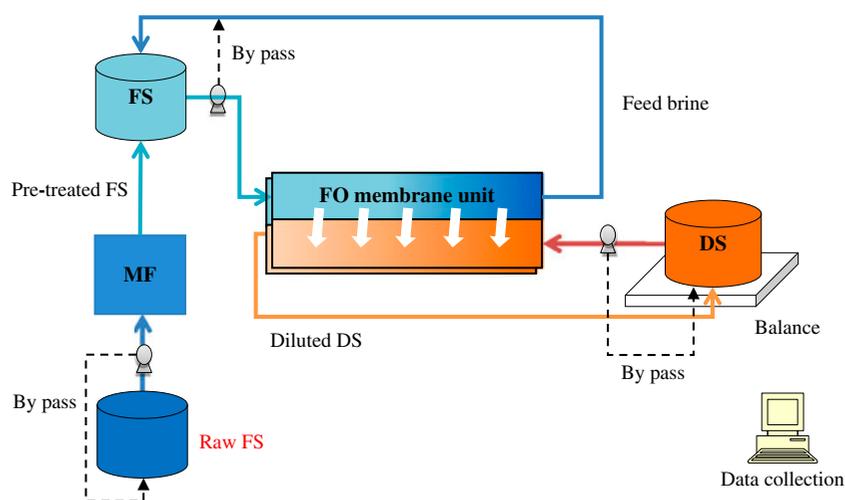
Fig. 2. Schematic diagram of pilot-scale FDFO desalination system.

was employed as a post-treatment. This study, however, focused only on the evaluation of the performances of the two SWFO modules and the NF process, which was already reported in our earlier study [16].

The volumetric water flux was determined by measuring the change in mass of the DS tank during the operation. The change of mass of the DS tank was automatically recorded by connecting to a data-logging computer. The water flux of both FO modules was calculated by [17]:

$$J_w = \frac{\text{Change in permeate weight (L)}}{\text{Effective membrane area (m}^2) \times \text{Time (h)}}$$

3. Results and discussion

3.1. Baseline performance of 8040 SWFO membrane modules

According to the membrane module supplier, the expected water flux of the clean membrane module is 8 ± 2 (Lm^{-2}h^{-1}) using 5% NaCl as DS with tap water as FS. The permeate fluxes of both CS and MS modules obtained in this study are presented in Fig. 3. The average water flux for the CS module was about 35% higher than that of MS module. There are two possible causes of this higher water flux for the CS module. CS module has a larger volumetric space provided by the thicker CS in the channel. Although the initial water flux at the inlet point of the channel might be similar to both the modules, however, along the length of the channel, the average water flux would differ. This is because the extent of the dilution of the DS is different from each module and is affected by the volume of the DS present in the channel. Since a larger spacer volume is present for CS module with lower

membrane area, the extent of dilution of the DS in the channel is slightly lower than that of the MS module. This results in slightly higher bulk DS concentration gradient along the channel for CS module. Although the cross-flow velocity is expected to be higher for MS module, however, this has no implications on the water flux because the feed water used was tap water (no external concentration polarization [ECP] is present). Moreover, the DS faces the membrane support layer and is not affected by the cross-flow velocity in reducing the dilutive CP. Therefore, spacer thickness plays a significant role in the average water flux and this has been observed in other studies [8,18–20]. It was observed that the initial water flux of CS module was around 50% higher than that of MS module although both contain the same type of CTA membrane. This higher water flux in the initial stage is likely due to the duration required for each module to get stabilized. From this result, it is apparent that it takes more time for CS module to reach a stable flux. In the following section, the effect of adjustable operating conditions on the performances of both CS and MS modules are discussed.

3.2. Flux behavior under different feed flow rates

The influence of feed flow rates on the water flux for CS and MS modules was evaluated by operating the modules at different feed flow rates: 50, 70, and 100 LPM (3, 4.2, and 6 m^3/h, respectively). The pressure difference between the ends of the feed channel module and the difference between the DS and FS channels were controlled as per the manufacturer's recommendation. Based on the previous experimental study of pilot-scale 4040 SWFO module [7], the feed pressure of both FO modules was constant at less than 1 bar during all experiments, and it was concluded that the feed flow rate should be higher than the draw flow rate because of the pressure drop through the
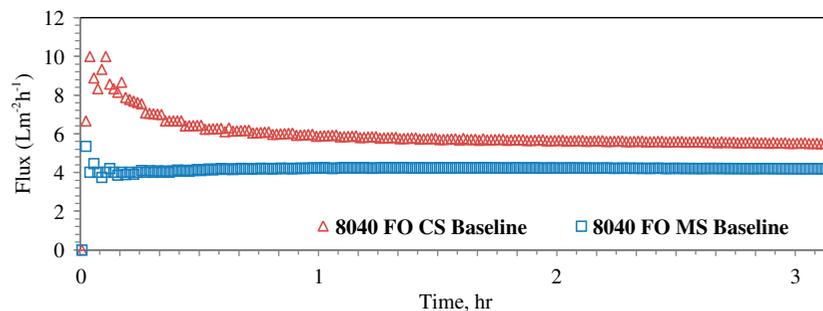
Fig. 3. Water flux data in both FO modules using pre-treated tap water and 5% NaCl as FS and DS, respectively. Feed and DS flow rates were maintained at 50 and 0.5 LPM, respectively.

membrane [7]. Higher DS flow rate could undermine the integrity of the FO membrane due to pressure on the support layer side of the membrane.

The feed flow rates in this study were constant at 50, 70, and 100 LPM, while the draw flow rate was maintained at 0.5 LPM. The DS flow rate was determined based on the pressure of DS at the channel inlet. As per the supplier's recommendation, the pressure should not be more than 0.7 bar at the inlet and 0.15 bar at the outlet of the DS channel. This pressure rating has been recommended to protect the active layer of the FO membrane on the other side of the support layer from delamination due to the hydraulic pressure created in the DS chamber.

As shown in Fig. 4, the feed flow rates have an obvious influence on the water flux for both FO membrane modules. The water flux of both modules showed a similar behavior at feed flow rate of 50 LPM. At this lowest cross-flow rate (i.e. 50 LPM), the water flux was almost constant even after 5 h of operation for both the modules although the water flux for CS module was slightly higher than MS module. In the earlier studies, the water flux of the membrane increased with increase in the feed flow rate [3,6,7,21]. When the feed flow rates were increased to 70 and 100 LPM, the water flux also increased for both FO membrane modules. As shown in Fig. 4, however, the increase in the flux decline with time was observed when the modules operated at higher feed flow rates. In addition, the water flux for CS module was consistently higher than the MS module for all the feed flow conditions.

The increase in water flux at higher feed flow rates is likely caused by increase in the cross-flow velocity shear force at the membrane surface that helps in reducing the impact of ECP. The increase in cross-flow velocity improves the mass transfer coefficient of the feed and ultimately results in improved water flux across the membrane. Moreover, at higher feed flow

rates, the modules operate at much lower feed recovery rates and hence the average bulk feed concentration within the module remains proportionately lower resulting in greater net driving force and higher average water flux in the module.

The higher water flux observed for CS module than the MS module for all the conditions tested in Fig. 4 could be caused by several reasons. The first one is because of the higher volume of CS channel, which results in lower dilution of the DS in the channel as already explained in the earlier section. The other reason is also due to lower feed recovery rate for CS module because of the lower membrane area in comparison to MS module. As the membrane area is increased, the feed recovery rate also increases at the module outlet which in turn decreases the osmotic gradient of the module channel. Likewise it also increases the bulk dilution factor of the DS at the module outlet. This eventually reduces the average net driving force of the module resulting in lower water flux for module. This behavior is expected to be true for most cases for FO process operated with larger membrane area even though the modules may have a similar spacer design [9]. Similar behavior on the average water flux has been observed for pressure-based membrane such as the RO membranes [22,23].

The other potential cause of higher water flux with the CS module is the influence of a feed spacer design. The SW module has been developed to allow the fluid to mix well by creating turbulent hydrodynamic conditions. The hydrodynamics in the SWM feed channel are influenced by the spacer properties resulting in the increase of the effective flow velocities [10]. It has been found that the mass transfer in the membrane in the channel increases when the membrane module with the higher spacer height is used. Further, the CS not only provides larger channel volume due to larger spacer thickness but also creates a more turbulent flow
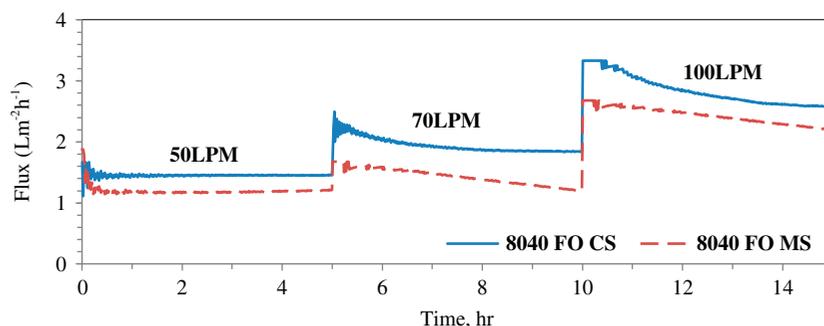
Fig. 4. Effect of feed flow rate on the water flux in both SWFO membrane modules. Experimental conditions: 0.6 M SOA DS and BGW5 FS, feed flow rates of 50, 70, and 100 LPM.

regime within the channel due to corrugated nature of the spacers thereby resulting in improved hydrodynamic conditions that prevents the fouling/scale potential of the feed water.

The flux decline observed in Fig. 4 at higher feed flow rate is caused by the increased water flux that results in more volume of water coming to the DS tank and achieving higher dilution factor of the DS since these experiments were conducted with the fixed initial DS volume. At 100 LPM, the flux decline is even sharper for CS module because of the highest water flux that results in the highest dilution factor of the DS amongst all the conditions tested in Fig. 4. The other potential cause of the flux decline in Fig. 4 could be attributed by the reverse diffusion of draw solutes that could react with some of the feed ions forming insoluble scales on the membrane surface. For example, if SO_4^{2-} ions pass through the membrane, it could react with Ca^{2+} ions present in the feed water to form insoluble gypsum ($CaSO_2$) that could reduce water flux. The flux decline can be caused by the rise in the total hydraulic resistance caused by the reverse diffusion of draw solutes into the feed side of the membrane [21] and the reduction of the driving force through the membrane caused by the concentrate FS and the diluted DS with time referred to as CP [24]. However, given the very low RSF observed for SOA in the earlier studies [12,25], the influence of gypsum scaling is not expected to be very significant at least in this study. Even if any scaling layer has been formed during the FDFO process, the physical cleaning would have easily removed because the baseline flux after each experiment and cleaning cycle was no different from the original baseline flux. The fouling behaviors and physical cleaning effects on water flux in lab-scale FO process have been investigated in the previous studies [21,26,27]. Unlike the RO process, the fouling layer formed in the FO process is loosely compacted due to the absence of hydraulic pressure. As a result,

the fouling layer in the FO process can be easily removed by physical cleaning. Therefore, operating pilot-scale FO membrane modules can offer an advantage of reducing the requirement for chemical cleaning procedure, and this leads to more or less requirement of chemical cleaning reagents.

3.3. Effect of SOA DS concentrations on the permeate flux

Fig. 5 shows the water flux of both FO modules as a function of the operating time using different DS concentrations (0.6, 0.8, and 1.0 M SOA). Clearly, higher water fluxes in both FO modules were observed at higher DS concentration. This is obviously due to higher driving forces created by the increased osmotic pressure difference between the two solutions when higher DS concentration is used. This trend has been reported in many earlier studies both in the lab-scale and larger-scale studies although the correlation between the DS concentration and the water flux has been observed to non-linear due to the enhanced influence of dilutive internal CP at higher DS concentrations [3,5,12,24,28]. In Fig. 5, although increasing the DS concentration improved water flux, the flux decline in MS module was clearly observed when higher DS concentrations were used. This increased flux decline at higher DS concentrations can be explained as higher DS dilution factor achieved the similar phenomenon already discussed earlier. At higher water flux, more volume of water gets accumulated on the DS tank, which reduces the bulk DS concentration more since a fixed initial volume of DS was used. This results in sharper flux decline in both modules when higher DS concentration (i.e. 1 M SOA) is used. It is interesting to note that the water flux for MS module dropped sharply after about 1 h of operation when 1 M DS concentration was used. This sharp decline of water flux is likely caused by the scaling at
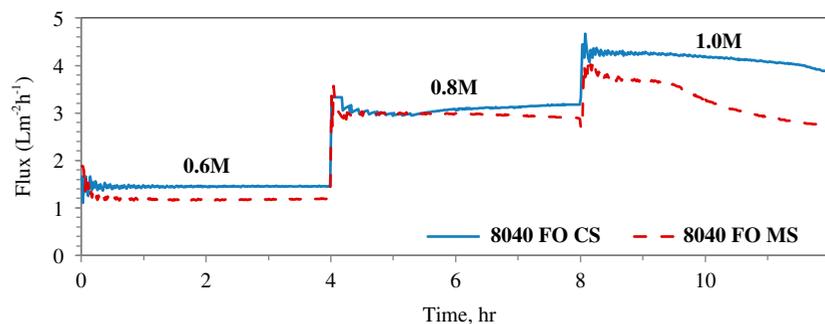
Fig. 5. Effect of SOA DS concentrations on the water flux in both SWFO membrane modules. Experimental conditions: 0.6, 0.8, and 1.0 M SOA DS and BGW5 FS, feed flow rate of 50 LPM.

the membrane surface due to reverse diffusion of draw solutes toward the feed water. This phenomenon was not observed in Fig. 4 due to the lower DS concentration used (0.6 M SOA). When the DS concentration was increased to 1 M SOA, the reverse solute flux also increased proportionately and hence the influence of scaling compounds such as gypsum on the water flux could have become significant. This sharp decrease in the water flux was not observed for CS module, and this may likely be due to the turbulence regime created by the CS design in the feed channel which prevented the gypsum scales from attaching the membrane surface.

According to the previous studies [8,19,23,29], the spacer plays an important role in mass transfer coefficient through the membrane by increasing velocity shear and turbulence inside the feed channel. Schwinge et al. [8] pointed out that the optimization of many factors such as spacers, leaf geometry, and operating conditions is important to enhance the performance of SWM. As previously mentioned, the spacer in CS module is different from that in MS module; consequently, the results indicated that the corrugated spacer in CS module can help to achieve higher water flux than MS module because of the more turbulent flow regime created by the CS.

3.4. Effect of TDS of the BGW on the permeate flux

In our previous work, we carried out the experiment using 1 M SOA as DS and the simulated BGW as FS; as a result, the water flux was around 9 and $5 \, Lm^{-2} h^{-1}$ with BGW 5 and 35, respectively [15], indicating that the net driving force across the membrane was obviously influenced by the feed TDS concentration in the FO process [15]. The influence of feed property on the water flux was observed by varying the feed TDS (BGW5, BGW10, and BGW35

representing TDS of 5,000, 10,000, and 35,000 mg/L) while maintaining a constant DS concentration (i.e. 1.0 M SOA). Fig. 6 indicates that, as the feed TDS concentration was increased, the water flux significantly decreased for both the FO modules, and these results are in good agreement with other previous results [15,30].

In general, the performance of CS module was slightly better than that of MS module in terms of the water flux. The water flux for the CS module was higher but the decline with time was moderate in comparison to MS module, where the flux was lower and the flux decline was relatively shaper and more significant.

The cause of the higher water flux for CS module is similar to the reasons already explained earlier. The sharp decline in water flux for MS module was also explained as likely caused by the scaling of the membrane due to reverse diffusion of draw solutes. However, when a feed with higher TDS was used (BGW10 and BGW35), the sudden sharp fall in the water flux observed with BGW5 was not observed anymore. This is because as the feed TDS was increased, the concentration gradient also decreased at the same DS concentration. Since the reverse solute flux or the reverse diffusion of draw solute is a function of the concentration gradient [3,31], it is expected that the reverse solute flux will decrease with the increase in feed TDS ultimately lowering the prospects of forming scales on the membrane surface. This results in more uniform flux decline at higher feed TDS although the water flux for the CS module was higher than MS module and it had higher volumetric dilution of DS with time. However, the degree of flux decline was lower or more gradual for CS than MS module. This further shows the role of the corrugated feed spacer that creates higher turbulence in the feed channel and can help mitigate the accumulation of scales on the
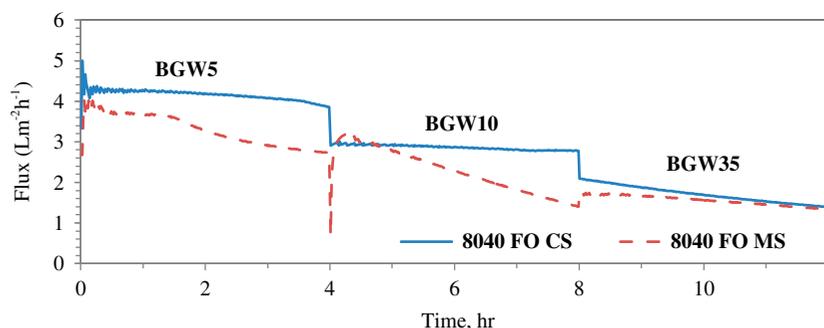
Fig. 6. Effect of feed TDS concentrations on the water flux in both SWFO membrane modules. Experimental conditions: 1.0 M SOA DS and FS of BGW5, 10, and 35, feed flow rate of 50 LPM.

membrane surface. The mass transfer enhancement is caused by higher local shear stress contributing to enhanced water flux in the membrane process [18,32].

4. Conclusions

Fertilizer-drawn FO desalination of BGW was investigated at a pilot-scale level using two different types of spiral-wound FO membrane modules and their performances were evaluated under different operating conditions. The following conclusions have been drawn from this particular study.

- The feed water flow rate had a positive influence on the water flux of the SWFO membrane module due to increase in mass transfer coefficient across the membrane that reduced the effect of ECP.
- Concentration of feed and DSs played a crucial role in the average water flux of the FO modules because they were directly related to the osmotic driving force across the membrane.
- The performance of CS module was slightly better than that of MS module in terms of water flux and scaling prevention thereby indicating the role of spacer design in the pilot-scale FO membrane modules. The CS module led to creating better hydrodynamic conditions within the channel that reduced not only the coupled effects of concentrative ECP and dilutive ICP but also the volumetric dilution of DS within the channel. This study, therefore, among other things showed the importance of spacer design and thickness of overall efficiency of the large-scale FO module.

References

[1] T. Cath, A. Childress, M. Elimelech, Forward osmosis: Principles, applications, and recent developments, J. Membr. Sci. 281(1–2) (2006) 70–87.
[2] S. Zhao, L. Zou, C.Y. Tang, D. Mulcahy, Recent developments in forward osmosis: Opportunities and challenges, J. Membr. Sci. 396 (2012) 1–21.
[3] N.T. Hancock, T.Y. Cath, Solute coupled diffusion in osmotically driven membrane processes, Environ. Sci. Technol. 43(17) (2009) 6769–6775.
[4] C.Y. Tang, Q. She, W.C.L. Lay, R. Wang, A.G. Fane, Coupled effects of internal concentration polarization and fouling on flux behavior of forward osmosis membranes during humic acid filtration, J. Membr. Sci. 354(1–2) (2010) 123–133.
[5] J.R. McCutcheon, R.L. McGinnis, M. Elimelech, A novel ammonia–carbon dioxide forward (direct) osmosis desalination process, Desalination 174(1) (2005) 1–11.
[6] Y. Xu, X. Peng, C.Y. Tang, Q.S. Fu, S. Nie, Effect of draw solution concentration and operating conditions on forward osmosis and pressure retarded osmosis performance in a spiral wound module, J. Membr. Sci. 348(1–2) (2010) 298–309.
[7] Y.C. Kim, S.J. Park, Experimental study of a 4040 spiral-wound forward-osmosis membrane module, Environ. Sci. Technol. 45(18) (2011) 7737–7745.
[8] J. Schwinge, P.R. Neal, D.E. Wiley, D.F. Fletcher, A.G. Fane, Spiral wound modules and spacers, J. Membr. Sci. 242(1–2) (2004) 129–153.
[9] W. Van der Meer, J. Van Dijk, Theoretical optimization of spiral-wound and capillary nanofiltration modules, Desalination 113(2–3) (1997) 129–146.
[10] E.C. Holland, F.K. Lesan, P.H. Knappe, High recovery spiral wound membrane element, US Patents CA1302904 C, 1989.
[11] L. Chekli, S. Phuntsho, H.K. Shon, S. Vigneswaran, J. Kandasamy, A. Chanan, A review of draw solutes in forward osmosis process and their use in modern applications, Desalin. Water Treat. 43(1–3) (2012) 167–184.
[12] S. Phuntsho, H.K. Shon, S. Hong, S. Lee, S. Vigneswaran, A novel low energy fertilizer driven forward osmosis desalination for direct fertigation: Evaluating the performance of fertilizer draw solutions, J. Membr. Sci. 375(1–2) (2011) 172–181.
[13] S. Phuntsho, H. Shon, S. Hong, S. Lee, S. Vigneswaran, J. Kandasamy, Fertiliser drawn forward osmosis desalination: The concept, performance and limitations for fertigation, Rev. Environ. Sci. Biotechnol. 11 (2012) 147–168.
[14] S. Phuntsho, H.K. Shon, T. Majeed, I. El Saliby, S. Vigneswaran, J. Kandasamy, S. Hong, S. Lee, Blended fertilizers as draw solutions for fertilizer-drawn forward osmosis desalination, Environ. Sci. Technol. 46(8) (2012) 4567–4575.
[15] S. Phuntsho, S. Hong, M. Elimelech, H.K. Shon, Forward osmosis desalination of brackish groundwater: Meeting water quality requirements for fertigation by integrating nanofiltration, J. Membr. Sci. 436 (2013) 1–15.
[16] J.E. Kim, S. Phuntsho, H.K. Shon, Pilot-scale nanofiltration system as post-treatment for fertilizer-drawn forward osmosis desalination for direct fertigation, Desalin. Water Treat. 51 (2013) 6265–6273.
[17] E.R. Cornelissen, D.J.H. Harmsen, E.F. Beerendonk, J.J. Qin, J.W.M.N. Kappelhof, Effect of draw solution type and operational mode of forward osmosis with laboratory-scale membranes and a spiral wound membrane module, J. Water Reuse Desalin. 1(3) (2011) 133–140.
[18] Z. Cao, D. Wiley, A. Fane, CFD simulations of net-type turbulence promoters in a narrow channel, J. Membr. Sci. 185(2) (2001) 157–176.

[19] J. Phattaranawik, R. Jiraratananon, A. Fane, C. Halim, Mass flux enhancement using spacer filled channels in direct contact membrane distillation, J. Membr. Sci. 187(1–2) (2001) 193–201.

[20] J. Fárková, The pressure drop in membrane module with spacers, J. Membr. Sci. 64(1–2) (1991) 103–111.

[21] S. Lee, C. Boo, M. Elimelech, S. Hong, Comparison of fouling behavior in forward osmosis (FO) and reverse osmosis (RO), J. Membr. Sci. 365(1–2) (2010) 34–39.

[22] W. Zhou, L. Song, T.K. Guan, A numerical study on concentration polarization and system performance of spiral wound RO membrane modules, J. Membr. Sci. 271(1–2) (2006) 38–46.

[23] G. Schock, A. Miquel, Mass transfer and pressure loss in spiral wound modules, Desalination 64 (1987) 339–352.

[24] J.R. McCutcheon, M. Elimelech, Influence of membrane support layer hydrophobicity on water flux in osmotically driven membrane processes, J. Membr. Sci. 318(1–2) (2008) 458–466.

[25] A. Achilli, T.Y. Cath, A.E. Childress, Selection of inorganic-based draw solutions for forward osmosis applications, J. Membr. Sci. 364(1–2) (2010) 233–241.

[26] S. Zhao, L. Zou, Effects of working temperature on separation performance, membrane scaling and cleaning in forward osmosis desalination, Desalination 278(1–3) (2011) 157–164.

[27] B. Mi, M. Elimelech, Organic fouling of forward osmosis membranes: Fouling reversibility and cleaning without chemical reagents, J. Membr. Sci. 348(1–2) (2010) 337–345.

[28] G.D. Mehta, S. Loeb, Internal polarization in the porous substructure of a semipermeable membrane under pressure-retarded osmosis, J. Membr. Sci. 4 (1978) 261–265.

[29] J.D. Mannapperuma, Corrugated spiral membrane module, US Patents 5458774A, 1995.

[30] J.R. McCutcheon, R.L. McGinnis, M. Elimelech, Desalination by ammonia–carbon dioxide forward osmosis: Influence of draw and feed solution concentrations on process performance, J. Membr. Sci. 278(1–2) (2006) 114–123.

[31] W.A. Phillip, J.S. Yong, M. Elimelech, Reverse draw solute permeation in forward osmosis: Modeling and experiments, Environ. Sci. Technol. 44(13) (2010) 5170–5176.

[32] T. Chong, F. Wong, A. Fane, Implications of critical flux and cake enhanced osmotic pressure (CEOP) on colloidal fouling in reverse osmosis: Experimental observations, J. Membr. Sci. 314(1–2) (2008) 101–111.